Fig. S7

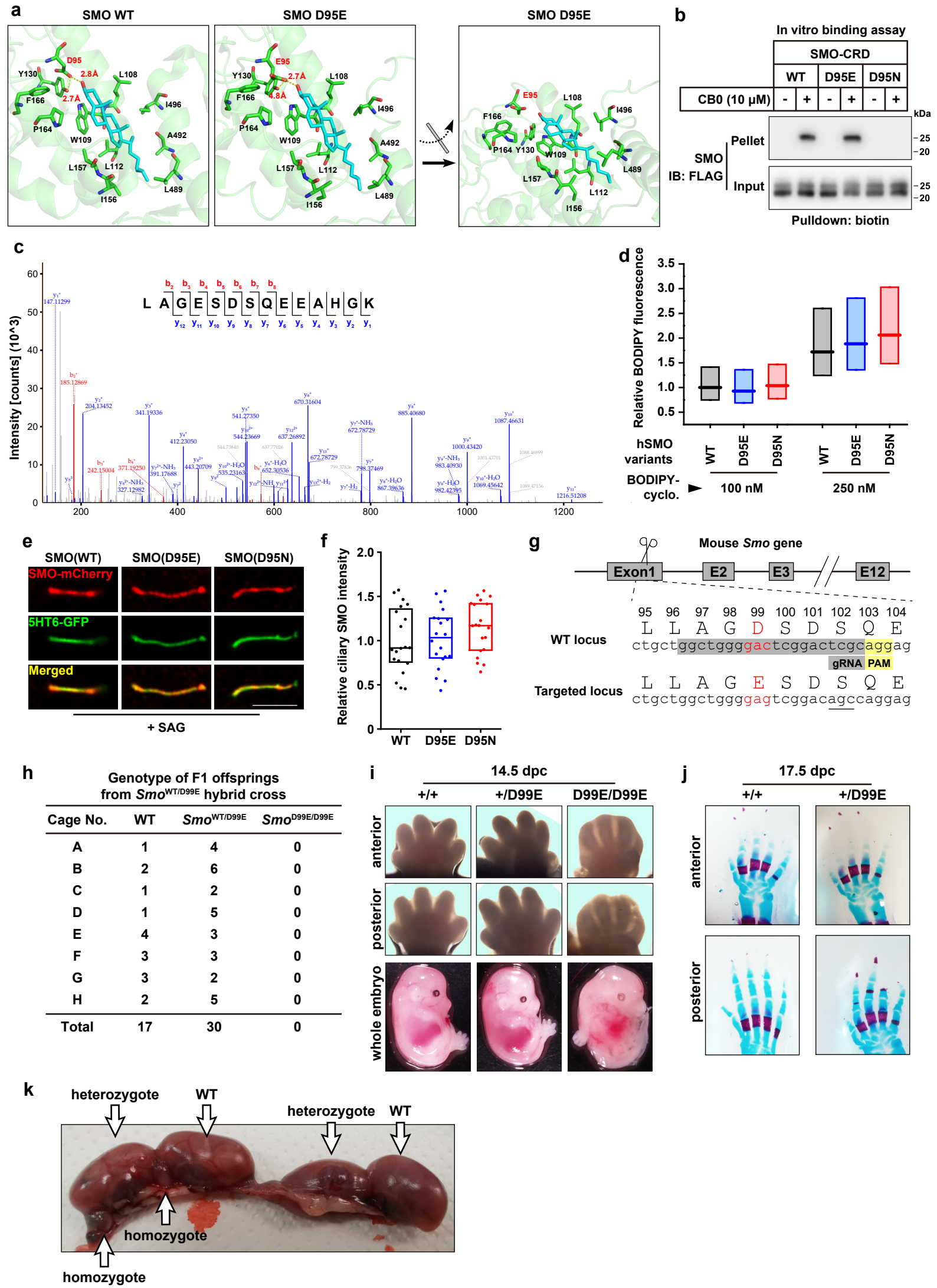

Cage No.	WT	*Smo*$^{WT/D99E}$	*Smo*$^{D99E/D99E}$
A	1	4	0
B	2	6	0
C	1	2	0
D	1	5	0
E	4	3	0
F	3	3	0
G	3	2	0
H	2	5	0
Total	17	30	0

Fig. S7. Characterization of SMO(D95E).

a. Amino acid substitution simulation of SMO(D95E) to dock cholesterol based on the structure of hSMO-cholesterol complex (PDB: 5L7D).

b. *In vitro* binding assay of the purified SMO-CRD variants with CB probe.

c. Mass spectrum of CRD(D95E). The parental ion of E95 was successfully detected and shown, while the cross-linked peptide of E95-Y130 was not detected.

d. Analysis of BODIPY-cyclopamine binding to SMO variants by flow cytometry. Horizontal lines denoted mean values, and boxes denoted 25^{th} (lower limits) and 75^{th} quantiles (upper limits).

e. SMO variants translocated to primary cilia in response to SAG. NIH3T3 cells expressing mCherry-tagged SMO variants and 5HT6-GFP were treated with 100 nM SAG for 1 hr, and fixed for confocal microscopy. Bar=3 μm.

f. Quantification of ciliary SMO intensity in e. n=20.

g. Strategy to generate *Smo* p.D99E knockin strain by CRISPR-Cas9. A synonymous mutation was introduced at Ser102 to facilitate gene editing and was underlined.

h. Genotype of $Smo^{WT/D99E}$ hybrid cross offsprings from 8 breeding cages.

i. Limb and embryo morphologies of 14.5 dpc embryos.

j. Alizarin red and alcian blue staining of limb digits of 17.5 dpc embryos.

k. The appearance of 17.5 dpc embryos and the corresponding genotypes. Embryonic remnants of homozygous mutants were carefully separated and used for DNA extraction.